2007

Physics of complex transverse susceptibility of magnetic particulate systems

Dorin Cimpoesu
University of New Orleans

Alexandru Stancu

Leonard Spinu
Universityof New Orleans

Recommended Citation
Phys. Rev. B 76, 054409 (2007)

Physics of complex transverse susceptibility of magnetic particulate systems

Dorin Cimpoesu*
Advanced Materials Research Institute (AMRI), University of New Orleans, New Orleans, Louisiana 70148, USA

Alexandru Stancu
Faculty of Physics, "Al. I. Cuza" University, Iasi 700506, Romania

Leonard Spinu†
AMRI, University of New Orleans, New Orleans, Louisiana 70148, USA
and Department of Physics, University of New Orleans, New Orleans, Louisiana 70148, USA
(Received 8 March 2007; published 6 August 2007)

Complex transverse susceptibility is a recent proposed method for the determination of anisotropy and volume distributions in particulate magnetic media. So far, only thermal fluctuations and rate-dependent damped dynamics of the magnetic moment have been identified as reasons for the existence of the imaginary transverse susceptibility. In this paper, we apply a more general approach to derive the complex transverse susceptibility, and we show that the hysteresis phenomenon is the most general concept behind the existence of complex transverse susceptibility. In this paper, the physical origins of the imaginary part of transverse susceptibility are analyzed: rate-independent hysteresis, viscous-type rate-dependent hysteresis, and thermal relaxation effect origin. The rate-independent origin is an intrinsic contribution to the imaginary transverse susceptibility and cannot be neglected because it is a zero-temperature effect.

DOI: 10.1103/PhysRevB.76.054409 PACS number(s): 75.30.Gw, 75.40.Mg, 75.50.Ss, 75.50.Tt

I. INTRODUCTION

One of the important topics of condensed matter physics is the magnetism of nanostructured materials as ordered arrays of magnetic nanoparticles and nanowires, nanolithographically patterned structures, and multilayers. To reveal the properties of such systems, especially magnetic anisotropy, one needs appropriate experimental techniques.

Transverse susceptibility (TS) is one of the most sensitive methods in determining the magnetic anisotropy, and it was used with great success to characterize close-packed arrays of monodisperse Fe nanoparticles,[1] Fe(001) square nanostructures,[2] exchange-biased IrMn/FeCo multilayers,[3] epitaxial CrO_2 and CrO_2/Cr_2O_3 bilayer thin films,[4,5] and perpendicular recording media. Also, there is a great interest in describing theoretically the transverse susceptibility in magnetic nanosized systems.[6]

However, after almost 100 years since Gans[7] published his paper where the concept of transverse susceptibility was first discussed and in spite of many efforts dedicated to its study, the phenomenon of transverse susceptibility in magnetic systems is still not fully understood. The starting point in the way for experimental use of TS was the theoretical paper of Aharoni *et al.*[8] where the differential reversible susceptibility tensor of a magnetic system subject to coherent rotation magnetization processes was first calculated. The diagonalized susceptibility tensor includes the longitudinal and the two transverse components of the susceptibility with respect to the applied magnetic field. Thirty more years passed until Pareti and Turilli[9] experimentally verified the theory of Aharoni *et al.*[8] which predicted that the plot of TS versus applied field presents characteristic peaks located at the anisotropy and switching fields. Subsequently, as TS was more frequently used as a method for magnetic anisotropy investigations, the interest for TS grew exponentially and many studies contributed to the improvement of both theory and experimental method. Thus, some of the restrictions in the first theoretical approach of Aharoni *et al.*[8] were overcome[10–15] and the increased sensitivity of new experimental TS methods allowed the investigations of magnetic systems with very low concentration of magnetic moments.[3,4,16,17] A very recent development of TS constitutes the complex TS. It was first mentioned by Papusoi[18] in the context of magnetic particulate systems and it spurred a lot of attention as it was presented as a new way to determine the particle volume and anisotropy field distributions of a particulate medium.[19–23] The complex TS as calculated in Ref. 18 is a consequence of thermal relaxation of system's magnetic particles, whose relaxation rate can be controlled by the externally applied dc field and not by temperature as in the case of ac susceptibility.[24]

In this work, we apply a more general approach to derive the complex TS. We show that the imaginary part of TS can have three main origins which include those of Refs. 14 and 18. The starting point of our approach is the observation that the existence of an out-of-phase component of TS is essentially associated with a lag of the output (magnetization) with respect to the input (applied magnetic field). Etymologically, this lag between the effect and its cause corresponds to the word "hysteresis," and as it is shown in the following, the hysteresis phenomenon is the more general concept behind the existence of complex TS. In studying the hysteresis in magnetism, Bertotti[25] showed that the hysteresis can be understood using different ideas as lag, dissipation, memory and branching, or metastability. As defined in Ref. 25, the hysteresis is "the whole set of intimately connected phenomena arising from the simultaneous existence of metastable states, dissipation, mechanisms with characteristic time scales, and thermal relaxation." Analyzing the correspondence between metastability and hysteresis, it can be easily

observed that the metastability summarizes all the other interpretations of hysteresis. Various types of hysteresis can appear in a system with a complicated free-energy landscape featuring many local minima corresponding to metastable states. The main situations that can occur are rate-independent hysteresis, viscous-type rate-dependent hysteresis, and thermal relaxation. In the case of TS, so far, only the last two approximations were used to explain the occurrence of an imaginary part, i.e., viscous-type rate-dependent hysteresis in Ref. 14 and thermal relaxation in Ref. 18. These two situations will be revised in this paper in Secs. IV and V, where certain clarifications and corrections will be made. Before this, in Sec. III, the rate-independent hysteresis origin of the complex TS will be presented and analyzed. This is an intrinsic contribution to the complex TS being a zero-temperature approximation.

II. MAGNETIC SUSCEPTIBILITY TENSOR

The magnetic susceptibility is a quantity which describes the capability of a magnetic material to magnetize in response to a magnetic field. The magnetic susceptibility χ is defined by the ratio between the induced magnetization of a magnetic sample and the inducing magnetic field, describing the material's response to an applied magnetic field. Taking into account that both magnetization and magnetic field are vectors, the magnetic susceptibility of a magnetic sample is not a scalar. Response is dependent on the state of the sample and can occur in directions other than that of the applied field. To accommodate this, a general definition using a second rank tensor derived from derivatives of components of magnetization $\mathbf{M}$ with respect to components of the applied field $\mathbf{H}$:

$$\chi_{ij} = \frac{\partial M_i}{\partial H_j},$$

called the differential susceptibility, describes ferromagnetic materials, where i and j refer to the directions (e.g., x, y, and z in Cartesian coordinates) of the magnetization and applied field, respectively. The tensor thus describes the response of the magnetization in the ith direction from an incremental change in the jth direction of the applied field. Generally, the susceptibility tensor should comprise nine components, but, in fact, a maximum of three can be independent, because by appropriate choice of the orientation of the body-fixed coordinate system, the susceptibility tensor can be reduced to a diagonal form. The general tensorial character of the susceptibility is, in fact, related to the anisotropy of magnetic properties. The diagonalization of the susceptibility tensor takes place when the privileged directions of magnetization become parallel with the coordinate system's axis. If the change of the applied field provides only reversible change of magnetization (i.e., processes which involve no loss of energy), we have a reversible susceptibility.

In a differential susceptibility experiment, it is required to apply two magnetic fields: a dc bias field H_{dc}, which can be varied in a quite large range, and a small perturbing ac field H_{ac}, and the magnetization's variation is measured. The susceptibility is usually measured as the amplitude ratio of the first harmonic of the induced magnetization along a given direction and that of the ac field.

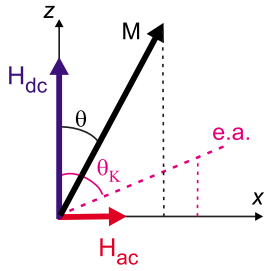

FIG. 1. (Color online) Transverse susceptibility experiment for a uniaxial single-domain ferromagnetic particle.

If the Oz axis is in the direction of the biasing dc field, then the diagonal elements of the tensor are the parallel susceptibility χ_{zz} measured in the field direction and the two transverse susceptibilities χ_{xx} and χ_{yy} measured perpendicular to the field direction.

III. TS IMAGINARY PART: RATE-INDEPENDENT HYSTERESIS EFFECT

Rate-independent hysteresis is a zero-temperature approximation where the system indefinitely remains in the local free-energy minimum which is initially occupied by the system.

In this approximation, let us consider that the dc field $\mathbf{H}_{\mathrm{dc}}$ acts along the Oz axis of a rectangular coordinates system and the ac field $\mathbf{H}_{\mathrm{ac}}=\mathbf{H}_{\mathrm{ac,max}}\sin \omega t$ acts along the Ox axis (see Fig. 1). Let us consider a spherical particle whose magnetization $\mathbf{M}$ reverses by coherent rotation, $|\mathbf{M}|=M_s$ by assumption and M_s is the saturation magnetization, having the volume V and the uniaxial anisotropy of constant $K>0$, with the easy axis in the xOz plane making the angle θ_k with the Oz axis. For low values of the ac field frequency, it may be assumed that the processes leading to a certain value of $\mathbf{M}$ have characteristic relaxation times much shorter than the time scale over which $\mathbf{M}$ varies significantly and the system approaches equilibrium; that is, the magnetization $\mathbf{M}$ lies in a minimum of the free energy at any moment, as in the theory of Aharoni *et al.*[8] Because of symmetry reasons, $\mathbf{M}$ will lie in the xOz plane. If the orientation of the magnetization is defined by spherical coordinate θ, then the particle's free energy is

$$E = -2KV\left[h_{\mathrm{dc}}\cos\theta + h_{\mathrm{ac}}\sin\theta + \frac{1}{2}\cos(\theta-\theta_k)^2\right], \quad (1)$$

where $h_{\mathrm{dc}}=H_{\mathrm{dc}}/H_k$, $h_{\mathrm{ac}}=H_{\mathrm{ac}}/H_k$, and $H_k=2K/\mu_0 M_s$ being the particle's anisotropy field. In the following, we will refer only to the behavior of the TS near the positive saturation, that is, $\theta\in(-\pi/2,\pi/2)$. The dependence of the particle's free energy on the magnetization's orientation is presented in Fig. 2 for two orientations of the easy axis.

If the particle's easy axis is perpendicular to the direction of the dc field ($\theta_k=90°$), then in the absence of the ac field, the free energy (1) shows one minimum for $h_{\mathrm{dc}}\geq 1$, located at $\theta=0$, and two minima for $-1<h_{\mathrm{dc}}<1$, located at θ_1^0

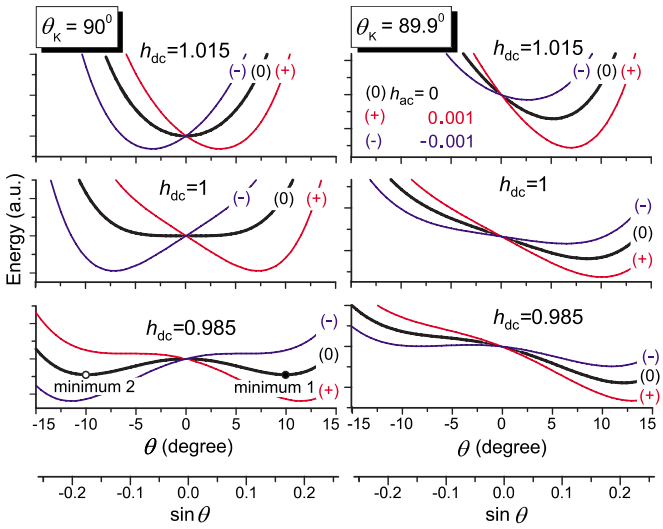

FIG. 2. (Color online) The particle's free energy [Eq. (1)] for $\theta_k=90°$ (left) and $\theta_k=89.9°$ (right).

$=\cos^{-1} h_{dc}$, referred hereafter as minimum 1, and $\theta_2^0 = -\cos^{-1} h_{dc}$, referred hereafter as minimum 2 (see Fig. 2). In the classical theory in which the amplitude of the ac field tends to zero, the magnetic moment oscillates reversibly around one of the two minima. If $h_{dc}=1$, the first nonvanishing derivative at the minimum point is of the order 4, else is of the order 2. So, for $h_{dc}=1$, the minimum is the broadest, and any arbitrary ac field, however small, will cause an oscillation of the magnetic moment and consequently the theory of Aharoni *et al.*[8] predicts a singular point of the TS at $h_{dc}=1$. However, in any experiment, the amplitude of the ac field is not zero in the mathematical sense and no singularity occurs at $h_{dc}=1$, and what is important to observe is that the peak of the TS occurs at a field $h_{dc}<1$ because the magnetic moment oscillates around the Oz axis between the minimum corresponding to $h_{ac}=h_{ac,max}$ and, respectively, $h_{ac}=-h_{ac,max}$ and not only around one of the two minima corresponding to $h_{ac}=0$ (see Fig. 2).

For a particle with $\theta_k=89.9°$, the energy landscape is not symmetric with respect to the Oz axis, as in the previous case. It can be seen in the Fig. 2 that for $h_{ac,max}=10^{-3}$, the magnetic moment oscillates only on the side $\theta>0$. A maximum of the TS occurs for a field $h_{dc}>1$, but the "distance" between the two minima is considerably smaller than in the case $\theta_k=90°$ so that the amplitude of the TS signal is much smaller. Consequently, for an ensemble of particles with a distribution of the orientation, the most important contribution to the TS comes from the particles with the easy axis oriented exactly perpendicular to the dc field, for which the energy plot is symmetric. In this sense, the affirmation that "the field dependence of TS presents a characteristic peak located at the anisotropy field" must be understood, and not that for any particle's orientations the TS presents a peak at $h_{dc}=1$. Increasing the amplitude of the ac field, the magnetic moment will have sufficient energy to oscillate on both sides of the Oz axis and the maximum of the TS occur at a field $h_{dc}<1$.

If

$$\frac{dE}{d\theta}=0,$$

$$\frac{d^2E}{d\theta^2}>0, \tag{2}$$

then the magnetic moment lies in a minimum of the free energy. The first condition can be written as a polynomial equation of fourth order in $\tan(\theta/2)$ which has explicit solutions, but it is rather difficult to choose the solutions which satisfy the second condition. To simplify the discussion, we shall use that $m_{ac}=\sin\theta$ is the normalized induced signal along the ac field direction, and then Eq. (2) can be written as

$$h_{ac}=f(m_{ac},\theta_k),$$

$$\frac{\partial f}{\partial m_{ac}}>0, \tag{3}$$

where

$$f(m_{ac},\theta_k)=h_{dc}\frac{m_{ac}}{\sqrt{1-m_{ac}^2}}+m_{ac}\cos 2\theta_k-\frac{1-2m_{ac}^2}{2\sqrt{1-m_{ac}^2}}\sin 2\theta_k. \tag{4}$$

The behavior of $f(m_{ac},\theta_k)$ as a function of m_{ac} for fixed θ_k is shown in Fig. 3. Its profile can be decomposed into two stable branches where $\partial f/\partial m_{ac}>0$, one for $m_{ac}<m_{ac,2}$ and the other for $m_{ac}>m_{ac,1}$, and a central unstable branch where $\partial f/\partial m_{ac}<0$. If $h_{ac,1}^c<h_{ac}(t)<h_{ac,2}^c$ for all t, then the change of the magnetic moment is reversible on one of the two stable branches. Otherwise, the right branch is traversed when h_{ac} decreases from $h_{ac,max}$ at point $A_1=(h_{ac,1}^c,m_{ac,1})$ where the right branch ends and the system jumps to point $A_1'=(h_{ac,1}^c,m_{ac,1}')$ on the left branch. A similar description applies when h_{ac} increases from $-h_{ac,max}$. Plotting m_{ac} as a function of h_{ac}, we obtain the hysteresis loop shown in Fig. 4. We note that $\lim_{h_{ac,max}\to 0}(df/dm_{ac})^{-1}$ gives the transverse susceptibility from Ref. 8.

For $\theta_k=90°$, we have $-h_{ac,1}^c=h_{ac,2}^c=(1-h_{dc}^{2/3})^{3/2}$, and, consequently, if $1>h_{dc}\geqslant(1-h_{ac,max}^{2/3})^{3/2} \overset{\text{notation}}{=} h^*$, then the ac field provides sufficient energy to the moment to oscillate around the Oz axis (cases 1 and 2 in Fig. 5), else, if $h_{dc}<h^*$, then the magnetic moment oscillates only around one of the two minima, as in the theory of Aharoni *et al.*[8] (case 3 in Fig. 5). For $\theta_k=89.9°$, no sudden jumps occur for $h_{ac,max}=10^{-3}$ and the motion of the magnetic moment is reversible.

First we have calculated TS as

$$\chi=\chi_0\frac{m_{ac,max}-m_{ac,min}}{2h_{ac,max}}, \tag{5}$$

where $\chi_0=M_sV/H_k$, so that the normalized susceptibility χ/χ_0 does not depend on the volume or anisotropy. The periodic induced signal m_{ac} has a phase shift with respect to h_{ac}, but its maximum takes place at the same moment of time

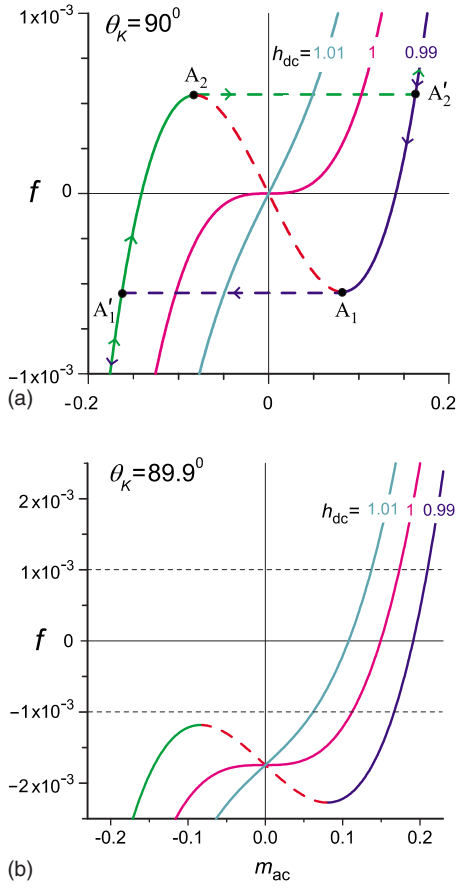

FIG. 3. (Color online) The profile of the function f [Eq. (4)] and genesis of hysteresis loop under alternating field excitation: (a) $\theta_k=90°$ and (b) $\theta_k=89.9°$. When h_{ac} decreases from $h_{ac,max}$, the system jumps from point $A_1=(h^c_{ac,1},m_{ac,1})$ to point $A'_1=(h^c_{ac,1},m'_{ac,1})$. When h_{ac} increases from $-h_{ac,max}$, the system jumps from point $A_2=(h^c_{ac,2},m_{ac,2})$ to point $A'_2=(h^c_{ac,2},m'_{ac,2})$.

with the maximum of the ac field (Fig. 5). Thus, relation (5) gives a real susceptibility. As the ac field amplitude increases, the position of the anisotropy peaks moves toward smaller field values, and the induced signal increases [Fig. 6(a)] but the TS decreases [Fig. 6(b)] because in Eq. (5) the

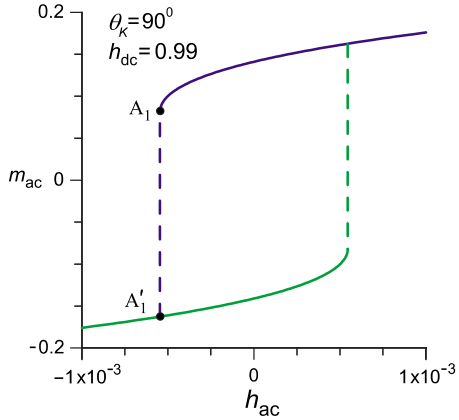

FIG. 4. (Color online) Hysteresis loop under alternating field for $\theta_k=90°$ and $h_{dc}=0.99$. The points A_1 and A'_1 are the same as in Fig. 3.

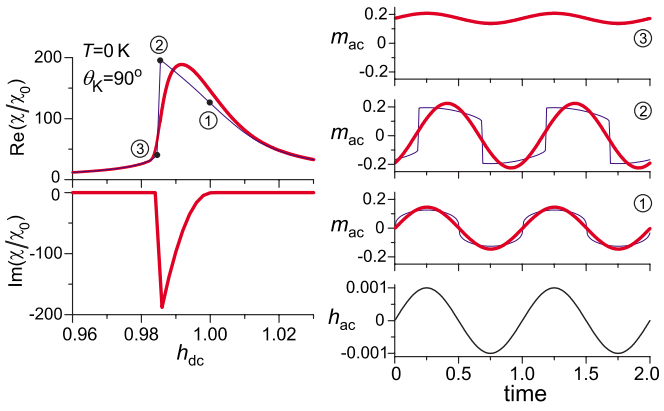

FIG. 5. (Color online) (Left) TS as a function of the dc field in the absence of the thermal fluctuations for $\theta_k=90°$, using extreme values [Eq. (5)] of the induced signal (thin line) and the first harmonic from the Fourier series (thick line); the ac field amplitude $h_{ac,max}=0.001$. (Right) Time evolution of the ac field h_{ac}, of the induced signal m_{ac} (thin line) and its first harmonic (thick line) at the points indicated in the first graph (time is normalized to the period of the ac field).

denominator increases much more than the numerator.

The experimental values reported in Refs. 19–22 are $H_{ac,max}=5-80$ Oe and $H_k=12$ kOe, namely, $h_{ac,max}=4.2\times10^{-4}-6.6\times10^{-3}$. So, we can easily see from Fig. 6 that ignoring the ac field amplitude can lead to systematic errors

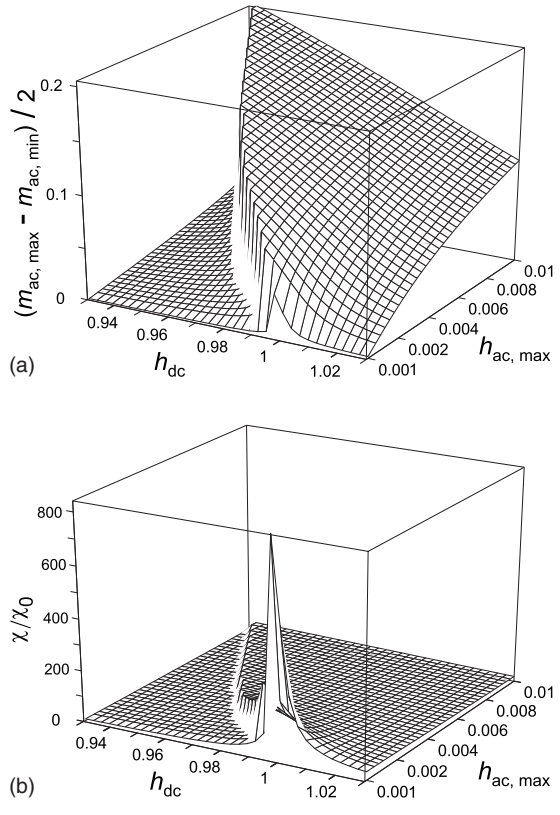

FIG. 6. (a) Induced signal and (b) TS as a function of the dc field and the ac field amplitude in the absence of the thermal fluctuations, calculated using extreme values of the induced signal [Eq. (5)] for $\theta_k=90°$.

in the evaluation of the anisotropy using TS experiments.

In Ref. 26, a perturbation approach was used to calculate the modification of magnetization due to a small ac field. The problem with the perturbation technique is that near the TS peaks, the variation $\delta\theta$ from Eq. (A3) (see the Appendix) is not a small deviation from equilibrium position θ^0, and, for example, the change in magnetization along the Oz axis cannot be approximated by $\sin\theta^0\delta\theta$.

Due to the rectangular-like form of the signal, its maximum is very difficult to be determined experimentally. So, we have analyzed the fitting with a sinusoidal function and, respectively, the calculus of the first harmonic from the Fourier series. Both methods give practically the same results for $\theta_k=90°$ and small differences otherwise. If the ac field is

$$H_{\rm ac}(t)=H_{\rm ac,max}\,{\rm Im}(e^{i\omega t})=H_{\rm ac,max}\sin\omega t,$$

where Im( ) denotes the imaginary part of the complex variable, then we define the magnetization $M(t)$ as a function of t by

$$M(t)=\frac{H_{\rm ac,max}}{V}\sum_{n=1}^{\infty}{\rm Im}(\chi_n e^{in\omega t})$$

$$=\frac{H_{\rm ac,max}}{V}\sum_{n=1}^{\infty}[\chi_n'\sin(n\omega t)+\chi_n''\cos(n\omega t)],$$

where $\chi_n=\chi_n'+i\chi_n''$ $(n=1,2,3,\ldots)$, and χ_n' and χ_n'' can be calculated by

$$\chi_n'=\frac{M_sV}{H_k}\frac{1}{h_{\rm ac,max}}\frac{2}{T}\int_0^T m_{\rm ac}(t)\sin(n\omega t)dt,$$

$$\chi_n''=\frac{M_sV}{H_k}\frac{1}{h_{\rm ac,max}}\frac{2}{T}\int_0^T m_{\rm ac}(t)\cos(n\omega t)dt.$$

Similar results are obtained if one uses

$$H_{\rm ac}(t)=H_{\rm ac,max}\,{\rm Re}(e^{i\omega t})=H_{\rm ac,max}\cos\omega t,$$

where Re( ) denotes the real part.

In Fig. 5, are presented the time evolution of the induced signal $m_{\rm ac}$ and its first harmonic for $\theta_k=90°$ and $h_{\rm ac,max}=0.001$. The first harmonic and the applied ac field are out of phase. Thus, we obtain an imaginary part of TS similar to the one described in Ref. 18, but independent of thermal relaxation.

The area of the loop described in the Fig. 4 measures the amount of energy dissipated during each excitation cycle (the energy loss per ac field cycle). Losses are solely hysteretic because we have assumed that the magnetization **M** lies in a minimum of the free energy at any moment. Actually, the dissipation takes place only in the Barkhausen jumps. The energy loss can be evaluated in terms of the imaginary part of the fundamental harmonic of susceptibility, as

$$\Delta E=\pi\mu_0H_{\rm ac,max}^2\chi_1''.$$

By construction, the loop area is equal to

$$\Delta E=2[E(m_{\rm ac,1},h_{\rm ac,1}^c)-E(m_{\rm ac,1}',h_{\rm ac,1}^c)],$$

where E is the particle's energy [Eq. (1)]. Now, we have

$$h_{\rm ac,max}^2\frac{\chi_1''}{\chi_0}=\frac{1}{\pi}\frac{E(m_{\rm ac,1},h_{\rm ac,1}^c)-E(m_{\rm ac,1}',h_{\rm ac,1}^c)}{K}.$$

That is, the product $h_{\rm ac,max}^2\chi_1''$ depends on the dc field only and does not depend on the ac field amplitude. When the dynamics is taken into account, due to the damping, a phase shift occurs between $h_{\rm ac}$ and $m_{\rm ac}$, so an imaginary component of TS also appears.[14]

Replacing ">" sign with "=" sign in Eqs. (2), we obtain

$$h_{\rm dc}\cos\theta_k+h_{\rm ac}\sin\theta_k=-\cos^3(\theta_k-\theta),$$

$$h_{\rm dc}\sin\theta_k-h_{\rm ac}\cos\theta_k=\sin^3(\theta_k-\theta),\qquad(6)$$

from which one further obtains

$$(h_{\rm dc}\cos\theta_k+h_{\rm ac}\sin\theta_k)^{2/3}+(h_{\rm dc}\sin\theta_k-h_{\rm ac}\cos\theta_k)^{2/3}=1.\qquad(7)$$

This equation gives the critical fields $h_{\rm ac,1}^c$ and $h_{\rm ac,2}^c$ where the Barkhausen jumps occur when $h_{\rm ac}$ decreases and increases, respectively.

When $h_{\rm ac}$ decreases, before the jump,

$$m_{\rm ac,1}=\sin\theta_1$$

$$=-\sin\theta_k(h_{\rm dc}\cos\theta_k+h_{\rm ac}\sin\theta_k)^{1/3}$$

$$-\cos\theta_k(h_{\rm dc}\sin\theta_k-h_{\rm ac}\cos\theta_k)^{1/3},$$

and after the jump,

$$m_{\rm ac,1}'=\sin\theta_1'=\frac{\tan(\theta_k-\theta_1')-\tan\theta_k}{\sqrt{(1+\tan^2\theta_k)[1+\tan^2(\theta_k-\theta_1')]}},$$

where

$$\tan(\theta_k-\theta_1)=-\frac{(h_{\rm dc}\sin\theta_k-h_{\rm ac,1}^c\cos\theta_k)^{1/3}}{(h_{\rm dc}\cos\theta_k+h_{\rm ac,1}^c\sin\theta_k)^{1/3}},$$

$$\tan(\theta_k-\theta_1')=-\tan(\theta_k-\theta_1)[1+\tan^2(\theta_k-\theta_1)$$

$$-\sqrt{1+\tan^2(\theta_k-\theta_1)+\tan^4(\theta_k-\theta_1)}].$$

By expressing the energy [Eq. (1)] in terms of $\tan(\theta_k-\theta)$, we find

$$\frac{\chi_1''}{\chi_0} = \begin{cases} \dfrac{1}{\pi h_{ac,max}^2}\left\{\dfrac{1}{2}\left[\dfrac{1}{1+\tan^2(\theta_k-\theta_1)} - \dfrac{1}{1+\tan^2(\theta_k-\theta_1')}\right] + \dfrac{1}{1+\tan^2(\theta_k-\theta_1)}\left[1+\sqrt{\dfrac{1+\tan^2(\theta_k-\theta_1')}{1+\tan^2(\theta_k-\theta_1)}}\right]\right\} \\ \qquad \text{if } (h_{dc}\cos\theta_k + h_{ac,max}\sin\theta_k)^{2/3} + (h_{dc}\sin\theta_k - h_{ac,max}\cos\theta_k)^{2/3} > 1 \\ 0 \qquad \text{elsewhere.} \end{cases} \tag{8}$$

Relations (6) and (7) can be better understood using the astroid formalism.[27,28] Assuming that the magnetization lies in a minimum of the free energy at any moment, its rotation is governed by the Stoner-Wohlfarth astroid (see Fig. 7). The standard procedure in the critical curve approach is to find the equilibrium orientation of the magnetization as the direction of the tangent to the critical curve passing through the tip of the total applied field vector (in our case, the sum between the $\mathbf{h}_{dc}$, with the origin in the astroid's center, and $\mathbf{h}_{ac}$). In Fig. 7, one sees in the critical curve approach how the amplitude of the ac field can induce the hysteretic processes described analytically for the particular case $\theta_k=90°$. For $h_{dc}\geqslant 1$, when h_{ac} decreases from $h_{ac,max}$ (point a in Fig. 7) to $-h_{ac,max}$ (point b), the tangency point shifts continuously from point a' to point b'; for $h_{ac}=0$, the tangency point is in the astroid's cusp, that is, the magnetic moment switches its direction into the negative sense along with the ac field. For $1>h_{dc}\geqslant h^*$, the vector $\mathbf{h}_{ac}$ cuts the astroid: when the extremity of the $\mathbf{h}_{ac}$ vector shifts from point a to point d, the tangency point moves continuously from a' to d; decreasing in continuance, the ac field from point d to point b, a jump will occur and the tangency point jumps into point d', from which it continuously shifts to b'. Increasing the h_{ac} from point b to point a, a jump will occur at point c where the tangency point will jump into point c'. For any arbitrary ac field, however small, there is an interval of the dc field for which the vector $\mathbf{h}_{ac}$ cuts the astroid and, as a result, a jump of the magnetic moment will occur. The angular interval in which the magnetic moment oscillates ($a'b'$ in Fig. 7) is maximum when the extremities of the vector $\mathbf{h}_{dc}+\mathbf{h}_{ac}$ are on the astroid, that is, $h_{dc}=(1-h_{ac,max}^{2/3})^{3/2}$. For lower values of the dc field, $h_{dc}<h^*$, the vector $\mathbf{h}_{ac}$ does not cut the astroid and the tangency point shifts continuously between point a' and point b', no sudden jump of the magnetic moment occurs, and the amplitude of the induced signal suddenly decreases giving rise to a peak in the TS curve. Increasing the ac field amplitude, the position of the TS peak moves toward smaller dc field values.

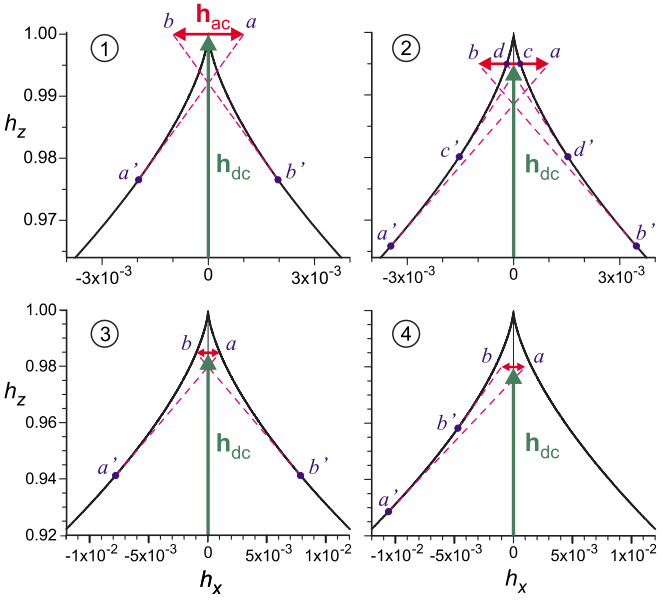

FIG. 7. (Color online) The astroid curve and the applied fields with $\theta_k=90°$, $h_{ac,max}=10^{-3}$, and different values of the dc field: (1) $h_{dc}=1$, i.e., the total applied field is in the exterior of the astroid and no sudden jump of the magnetic moment occurs; (2) $1>h_{dc}>(1-h_{ac,max}^{2/3})^{3/2}$, i.e., the vector $\mathbf{h}_{ac}$ cut the astroid; (3) $h_{dc}=(1-h_{ac,max}^{2/3})^{3/2}$, i.e., the extremities of the applied field are on the astroid, and the angular interval $a'b'$ in which the magnetic moment oscillates is maximum; and (4) $h_{dc}<(1-h_{ac,max}^{2/3})^{3/2}$, i.e., the vector $\mathbf{h}_{ac}$ does not cut the astroid and no sudden jump of the magnetic moment occurs.

IV. TS IMAGINARY PART: RATE-DEPENDENT HYSTERESIS EFFECT

In the previous section, the TS was derived without any reference to the rate at which the external field is varied. The role of the external field was only to bring the system to the point in which it becomes unstable and a spontaneous Barkhausen jump occurs. The spontaneous jump time scale is much shorter than the external field variation scale and, consequently, the evolution of the system was independent of the external field rate. However, rate-independent hysteresis is an approximation and real magnetization processes are rate dependent due to two main reasons.

First of all, Barkhausen jumps have a certain characteristic time scale determined by the processes on which the systems dissipates energy[25] as eddy currents or magnetization damping. Thus, for high field rate values, the system ceases to be described by spontaneous Barkhausen events and approaches a forced dynamic regime driven by the external magnetic field. In the present paper, we do not take into account the effect of eddy currents, and in Sec. IV A, we will analyze the occurrence of imaginary TS due the magnetization damping as a viscous-type rate-dependent hysteresis effect.

Second, as the temperature increases, the assumption that the system stays indefinitely in a local energy minima is not anymore valid and thermal triggered Barkhausen jumps can occur. These thermal effects have a certain time scale that

when correlated to the external field rate can determine an imaginary TS. This made the object of Ref. 18 and will be revised in Sec. IV B.

A. Viscous-type rate-dependent hysteresis

In the model presented previously, the TS is evaluated by employing a free-energy minimization method, namely, the model is frequency independent because it is assumed that in each moment the magnetization reaches an equilibrium state independent of the ac field rate. In real magnetic systems, the dynamics is associated with energy dissipation, determining a lag between the magnetization's response and the external excitation, which is strongly dependent on the excitation frequency. Consequently, knowing the frequency dependence of the TS becomes critical. The frequency used in the latest TS experimental setups has increased from kilohertz to megahertz[4] or even to gigahertz range,[29] so, it is important to have a model in which the frequency dependence of TS is taken into account. Moreover, owing to the damping at high frequency, a phase shift occurs between the applied ac field and the alternating magnetization; so, an imaginary component of TS appears.

A study of TS by focusing on magnetization dynamics is presented in Refs. 13 and 14. This model allows one to find a general formula for TS for any magnetic system if an expression for the magnetic free-energy density is known. The starting point of the model, as in the case of ferromagnetic resonance,[30] is the magnetization's equation of motion Landau-Lifshitz-Gilbert (LLG):[31]

$$\frac{d\mathbf{M}}{dt} = -\frac{|\gamma|}{1+\alpha^2}\mathbf{M}\times\mathbf{H}_{\text{eff}} - \frac{|\gamma|}{1+\alpha^2}\frac{\alpha}{M_s}\mathbf{M}\times(\mathbf{M}\times\mathbf{H}_{\text{eff}}), \tag{9}$$

where $|\gamma| = 2.211\times 10^5 (\text{rad/s})/(\text{A/m})$ is the gyromagnetic ratio, α is the Gilbert damping constant, and $\mathbf{H}_{\text{eff}}$ is the (deterministic) effective field and it incorporates the applied fields and the effects of different contributions in the free energy; the first term on the right-hand side of the LLG equation describes the gyromagnetic precession, and the second term describes the damping. The dynamics of the magnetization is governed by the relation that exists between the frequency of the external excitation and the frequency of resonance of the magnetic moment, which depends on the phenomenological damping term in the LLG equation. In order to preserve the magnetization's magnitude, the LLG equation can be expressed better in spherical coordinates (θ,φ), and the singularity of the spherical coordinates along the polar axis can be avoided by an adequate choice of the Oz axis. The dynamic susceptibility tensor in spherical coordinates is[14]

$$\chi_{\theta\varphi} = \frac{1}{\omega_r^2 - \omega^2 + i\omega\Delta\omega}\left(\frac{\gamma^2(1+\alpha^2)}{\mu_0}\begin{bmatrix} \dfrac{F_{\varphi\varphi}}{\sin^2\theta} & -\dfrac{F_{\theta\varphi}}{\sin\theta} \\ -\dfrac{F_{\theta\varphi}}{\sin\theta} & F_{\theta\theta}\end{bmatrix} + i\omega\gamma M_s\begin{bmatrix}\alpha & 1\\ -1 & \alpha\end{bmatrix}\right), \tag{10}$$

where

$$\omega_r = \frac{\gamma\sqrt{1+\alpha^2}}{\mu_0 M_s \sin\theta}\sqrt{F_{\theta\theta}F_{\varphi\varphi} - F_{\theta\varphi}^2}$$

and

$$\Delta\omega = \frac{\alpha\gamma}{\mu_0 M_s}\left(F_{\theta\theta} + \frac{F_{\varphi\varphi}}{\sin^2\theta}\right),$$

with $F_{\theta\theta}$, $F_{\theta\varphi}$, and $F_{\varphi\varphi}$ being the second derivatives of the free-energy density F at the equilibrium position (θ,φ) in the absence of the ac field. The susceptibility tensor in the laboratory system is given by

$$\chi_{xyz} = \mathbf{T}^t\cdot\chi_{\theta\varphi}\cdot\mathbf{T},$$

where

$$\mathbf{T} = \begin{bmatrix}\cos\theta\cos\varphi & \cos\theta\sin\varphi & -\sin\theta\\ -\sin\varphi & \cos\varphi & 0\end{bmatrix}.$$

From Eq. (10), we can see that the susceptibility tensor is related to the second derivative of the free-energy density F and is a measure of the "curvature" of F. We can also observe that the components of the susceptibility tensor are complex, the apparition of the imaginary part of TS being a direct consequence of the damping, in the absence of the damping the imaginary part being zero. So, an imaginary part of TS can occur even in the absence of thermal relaxation due only to the damping. Actually, thermal fluctuations and dissipation are related manifestations of one and the same interaction of the magnetic moment with its environment. We note that, however, this model does not take into account the amplitude of the ac field.

B. Thermal relaxation effect

Thermal relaxation is taken into account using a two-level model in Refs. 10 and 11 where only a real susceptibility is predicted, and it is shown that the temperature can change the position of the coercivity peak while the anisotropy peaks maintain their position, though their shape is altered. Monte Carlo simulations of the TS for a hexagonal array of dipolar interacting nanoparticles with random anisotropy are presented in Ref. 6, where only a real susceptibility is analyzed. However, the effect of the ac field amplitude is not discussed, even if in simulations $h_{\text{ac,max}} = 10^{-2}$ is taken and the obtained shift of the anisotropy peak toward lower field values is assigned only to thermal fluctuations. On the other hand, Papusoi[18] used also the two-level model, but an imaginary

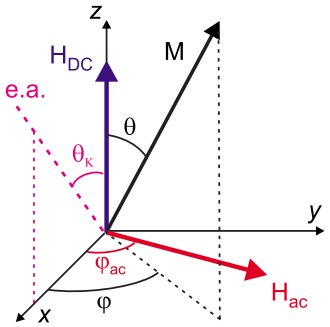

FIG. 8. (Color online) Sketch of the geometry used to calculate the complex TS.

TS is predicted because during a TS experiment, the increasing dc field shifts the particles' relaxation time toward lower values, making the occurrence of the thermal relaxation on the time scale of the ac field period possible. This mechanism is similar to that giving rise to a complex ac susceptibility,[24] where the role of the transverse field is played by the temperature. For a system of identical particles having the easy axis perpendicular to the dc field, the thermal relaxation gives rise to a secondary peak in the real part of the TS and to a peak in its imaginary part. The complex susceptibility is now used to separate volume and anisotropy field dispersions[19–22] by fitting the experimental data with the expressions obtained in Ref. 18.

In Ref. 23, the stochastic Landau-Lifshitz-Gilbert (SLLG) equation[32] is used in order to describe an array of 400 "Voronoi" cells with intergranular exchange and magnetostatic interactions, with different average diameters and dispersions, and a Gaussian anisotropy field distribution. It is shown that the volume dispersion only weakly affects the peak shape, according the model from Ref. 18, while the dependence on both anisotropy field dispersion and magnetization is substantial. The magnetostatic interactions distort the theory from Ref. 18, but the most substantial change is due to intergranular exchange. Recently, our micromagnetic analysis based on the SLLG equation showed a complex behavior of the real and imaginary parts of TS for a system of interacting particles.[33–35]

In the model presented in Ref. 18, the dc field acts along the Oz axis of a rectangular coordinates system and the ac field acts in the plane xOy, with the azimuth φ_{ac} (Fig. 8). Initially, a system of identical particle is taken into account. Each particle has the volume V and a uniaxial anisotropy of constant K, the easy axis being confined in the xOz plane, with the polar coordinate θ_k. The particle magnetization's spherical coordinates are denoted by (θ, φ). In order to better clarify the method used in Ref. 18 and because in Ref. 18 some typographical errors seem to be present, a detailed derivation of TS formula is exposed in the Appendix. Unfortunately, these errors propagated in the subsequent papers[19–23] dealing with the determination of volume and anisotropy field distributions in recording media using the model from Ref. 18.

The complex TS for a system of particles with the easy axis oriented perpendicular to the dc field direction ($\theta_k = 90°$) is given by (see the Appendix)

$$\chi_r = \begin{cases} \left(8\beta\kappa^2 \dfrac{1-h_{dc}^2}{\omega^2+4\kappa^2} + \dfrac{h_{dc}^2}{1-h_{dc}^2}\right)\cos^2\varphi_{ac} + \sin^2\varphi_{ac}, & h_{dc} < 1 \\ \dfrac{1}{h_{dc}-1}\cos^2\varphi_{ac}, & h_{dc} \geqslant 1, \end{cases} \tag{11}$$

$$\chi_i = \begin{cases} -4\omega\beta\kappa \dfrac{1-h_{dc}^2}{\omega^2+4\kappa^2}\cos^2\varphi_{ac}, & h_{dc} < 1 \\ 0, & h_{dc} \geqslant 1, \end{cases} \tag{12}$$

where $\kappa = f_0 \exp[-\beta(1-h_{dc})^2]$, f_0 is the attempt frequency and it is of the order of 10^9–10^{13} Hz, and $\beta = KV/k_BT$ is the thermal factor. In Ref. 18, Eq. (11) is approximated by

$$\chi_r = \begin{cases} 8\beta\kappa^2 \dfrac{1-h_{dc}^2}{\omega^2+4\kappa^2}\cos^2\varphi_{ac} + \sin^2\varphi_{ac}, & h_{dc} < 1 \\ \delta(h_{dc}-1)\cos^2\varphi_{ac}, & h_{dc} \geqslant 1, \end{cases}$$

where δ is the Dirac delta "function." However, this approximation does not give the correct variation of $\chi_r(h_{dc})$ in the proximate neighborhood of the point $h_{dc}=1$. For a particle system with volume and anisotropy field distributions,

$$\begin{aligned} \chi_{r0} = & \int_0^{h_{dc0}} \frac{1}{h_k} \frac{\cos^2\varphi_{ac}}{\dfrac{h_{dc0}}{h_k} - 1} G(h_k)dh_k \\ & + \int_{h_{dc0}}^{\infty} \left\{ 8\beta_0 \left[1 - \left(\frac{h_{dc0}}{h_k}\right)^2\right] \frac{1}{\bar{v}} \right. \\ & \times \left[\int_0^{\infty} \frac{\kappa^2}{\omega^2+4\kappa^2} v^2 F(v)dv \right] \cos^2\varphi_{ac} \\ & \left. + \frac{1}{h_k} \frac{\left(\dfrac{h_{dc0}}{h_k}\right)^2}{1 - \left(\dfrac{h_{dc0}}{h_k}\right)^2} \cos^2\varphi_{ac} + \frac{1}{h_k}\sin^2\varphi_{ac} \right\} G(h_k)dh_k, \end{aligned} \tag{13}$$

$$\begin{aligned} \chi_{i0} = & -4\beta_0\omega \frac{1}{\bar{v}} \cos^2\varphi_{ac} \int_{h_{dc0}}^{\infty} \left[1 - \left(\frac{h_{dc0}}{h_k}\right)^2\right] G(h_k) \\ & \times \left[\int_0^{\infty} \frac{\kappa}{\omega^2+4\kappa^2} v^2 F(v)dv \right] dh_k, \end{aligned} \tag{14}$$

where $h_{ac0} = h_{ac}/H_{k0}$, $h_{dc0} = h_{dc}/H_{k0}$, $h_k = H_k/H_{k0}$, $\chi_0 = \partial m_{ac}/\partial h_{ac0}$, $\beta_0 = K_0V_0/k_BT$, and $H_{k0} = 2K_0/\mu_0 M_s$ being the most probable value of the anisotropy field distribution, $G(h_k)$ is the normalized anisotropy field distribution, $v = V/V_0$, $\bar{v}$ is the mean normalized volume, V_0 is the most probable value of the particle volume distribution, $F(v)$ is the normalized particle volume distribution.

We note that in Ref. 18, the lower and upper limits of integrations in Eq. (13) are 0 and ∞, respectively, for both integral over anisotropy field distribution. Also, in Ref. 18, both lower limits of integration are equal to zero in Eq. (14) and β is used instead of β_0.

In the next section, these results are compared with the results obtained by numerical integration of stochastic Landau-Lifshitz-Gilbert equation, and an analysis of the influence of the ac field amplitude and of the interactions between particles on the complex TS method for the determination of volume and anisotropy field distributions in perpendicular recording media[19–22] is also presented.

V. LANGEVIN SIMULATION OF TS

In the presence of thermal agitation, it is supposed that the dissipative term from the LLG equation describes only the statistical (ensemble) average of rapidly fluctuating random forces and that for an individual particle the effective field must be augmented by a stochastic thermal field $\mathbf{H}_{\text{th}}$ which is assumed to be a normal (Gaussian) random process with the following statistical properties:[32]

$$\langle H_{\text{th},i}(t)\rangle = 0,$$

$$\langle H_{\text{th},i}(t)H_{\text{th},j}(t')\rangle = 2D\delta_{ij}\delta(t-t'),$$

$$D = \frac{\alpha k_B T}{\gamma \mu_0 M_s V},$$

where $\langle\rangle$ means the statistical average over different realizations of the fluctuating field, and i and j are the Cartesian indices. The Kronecker δ_{ij} expresses the assumption that the different components of thermal field are uncorrelated and the Dirac δ expresses that $H_{\text{th},i}(t)$ and $H_{\text{th},j}(t')$ are correlated only for time intervals $t-t'$ much shorter than the time required for an appreciable change of $\mathbf{M}$ according to the equation (LLG) (i.e., the random thermal forces are reduced to a "purely random" process, with a "white" spectrum). The constant D measures the strength of the thermal fluctuations and it is determined on the grounds of statistical-mechanical considerations. For a particle system, it is also assumed that the fluctuating fields acting on different magnetic moments are independent. The stochastic field changes the deterministic motion of the magnetization into a random walk. As a result, the LLG equation is converted into a stochastic differential equation of Langevin type with multiplicative noise:[32]

$$\frac{d\mathbf{M}}{dt} = -\frac{|\gamma|}{1+\alpha^2}\mathbf{M}\times(\mathbf{H}_{\text{eff}}+\mathbf{H}_{\text{th}}) - \frac{|\gamma|}{1+\alpha^2}\frac{\alpha}{M_s}\mathbf{M}\times[\mathbf{M}\times(\mathbf{H}_{\text{eff}}+\mathbf{H}_{\text{th}})]. \quad (15)$$

In this paper, we integrate the stochastic Landau-Lifshitz-Gilbert (SLLG) equation numerically by means of the Heun numerical integration scheme.[36] No temperature dependences of the anisotropy constant and saturation magnetization are taken. The magnetic properties follow from averages

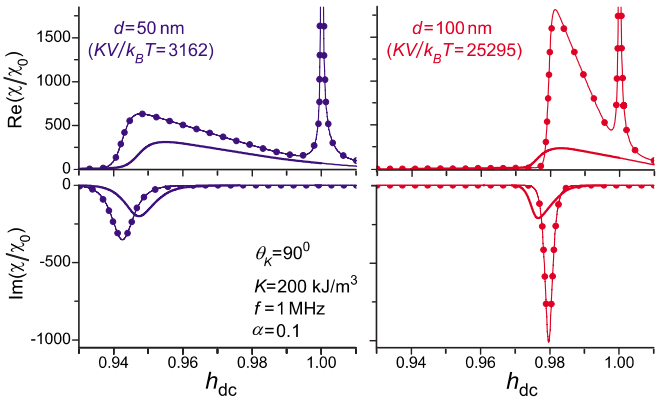

FIG. 9. (Color online) TS curves at $T=300$ K for two values of the particles' diameter, $d=50$ nm (left) and $d=100$ nm (right), obtained with the CP model (symbols) and SLLG with $h_{\text{ac,max}}=10^{-3}$ (line).

over many numerical realizations of the dynamic process. In order to test our program and to determine the time step size in numerical integration, we have considered a system of identical, noninteracting Stoner-Wohlfarth particles and we have compared our numerical results with the explicit solutions available in this case both for $T=0$ K and $T\neq 0$ K. The results obtained in this way are, in fact, identical to those calculated for one particle, because time average and average over the statistical ensemble are the same (ergodic hypothesis).

In our simulation, we have considered a system of 4096 noninteracting spherical particles, and the desired quantities are averaged over 10–30 cycles of the ac field, after the attenuation of the transitory effects which initially appeared. The results obtained by duplication of the number of particles practically coincide with the former, but the computation time increases significantly.

A. Identical particles

In Fig. 9, we compare our numerical results for a system of identical particles, obtained for $h_{\text{ac,max}}=10^{-3}$ and $\alpha=0.1$, with relations (11) and (12) obtained in Ref. 18 (referred hereafter as the CP model). The parameters' values used in the simulations are $M_s=300$ kA/m, $K=200$ kJ/m^3, $T=300$ K, $f=1$ MHz, and $\varphi_{\text{ac}}=0$. The results presented in Fig. 9 confirm the results of the CP model with certain differences, which can be explained in experimental conditions. However, as the SLLG method generates the stochastic trajectories for each individual magnetic moment, it provides much more insight into the dynamics of the system. The principal difference is that we do not obtain two peaks for the real part of TS due to no-vanishing amplitude of the ac field, while Eq. (11) always predicts two peaks, one of them being the anisotropy peak from the theory of Aharoni *et al.*[8], at $h_{\text{dc}}=1$. In our results, both the position and the amplitude of the TS peaks depend on $h_{\text{ac,max}}$, so that the comparison of these quantities between the two models is, in some ways, superfluous. However, we can see that for $\theta_k=90°$ and $h_{\text{ac,max}}=10^{-3}$, as the particles' diameter d increases, the real TS peak is always at higher values than that given by Eq.

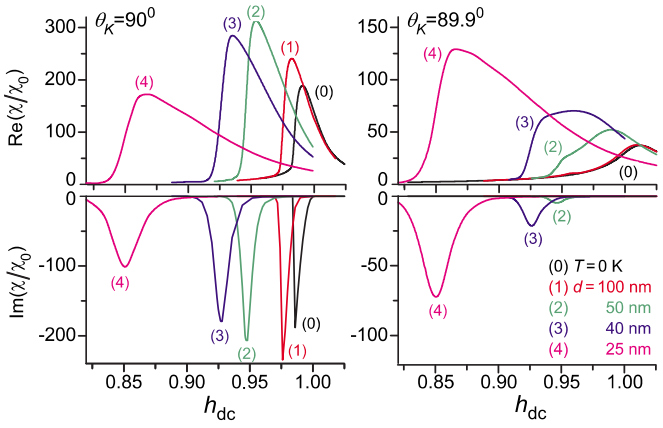

FIG. 10. (Color online) TS curves at $T=300$ K for different values of the particles' diameter d for $\theta_k=90°$ (left) and $\theta_k=89.9°$ (right). The curves for $T=0$ K are also presented for comparison.

(11), while the imaginary TS peak is moving from higher values to smaller values than that given by Eq. (12). In both models, an increase of the diameter d sharpens the TS peaks and shifts them to higher values of h_{dc}, but in our model, the amplitude of real TS as a function of particles' diameter has a maximum (see Figs. 10 and 11), while in Ref. 18, it is increasing toward an infinite value given by the theory of Aharoni *et al.*[8]

When θ_k decreases from 90°, both real and imaginary parts of the TS undergo a decrease (see Fig. 10 where the scale of the vertical axes for $\theta_k=90°$ is twice larger than that for $\theta_k=89.9°$). This decrease is very abrupt for the biggest particles but is smaller for the smallest particles because for these particles the effect of thermal relaxation is more important. Therefore, the TS is dominated by the particles having the easy axis perpendicular to the dc field ($\theta_k=90°$) only if the particles are sufficiently large.

In order to estimate the role of the temperature in the dynamics of the magnetic moment, we also present in Fig. 12 some typical time evolutions of the projection m_{ac} of the magnetic moment on the direction of the ac field. Due to the random character of the thermal fluctuations, the magnetic moment does not exactly follow a certain path on the energy surface, from one minimum to another one passing through the saddle point with the smallest energy barrier, like in the

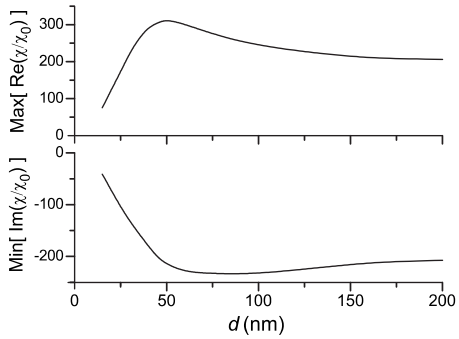

FIG. 11. The dependence of the maximum of the real part (up) and the minimum of the imaginary part (down) of TS on particles' diameter d.

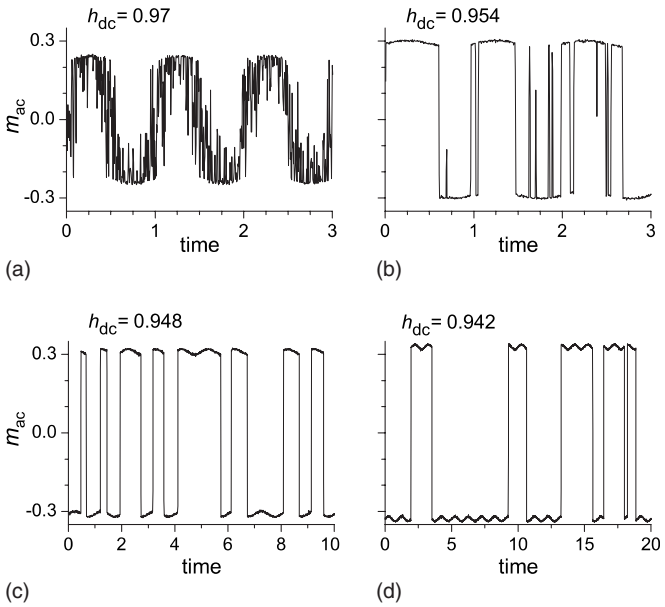

FIG. 12. Time evolution of the induced signal m_{ac} (time is normalized to the period of the ac field) for one particle with $d=50$ nm at $T=300$ K for $h_{ac}=0.001$, $\alpha=0.1$, and for different values of dc field: (a) $h_{dc}=0.97$, (b) $h_{dc}=0.954$, i.e., Re(χ) is maximum, (c) $h_{dc}=0.948$, i.e., Im(χ) is minimum, and (d) $h_{dc}=0.942$, i.e., the phase shift between m_{ac} and h_{ac} is maximum.

two-level model. In fact, there is always a probability for the magnetic moment to follow any other path, the path with the lowest energy barrier being the most probable. As we showed in Sec. III, if $h^* \leqslant h_{dc} \leqslant 1$ and $T=0$ K, then the ac field provides sufficient energy to the magnetic moment to oscillate around the Oz axis. For $T>0$ K, the magnetic moment effectuates random oscillations by thermal activation close to the bottom of the energy minima, but also a number of energy barrier crossings followed by a return to the original energy minima, from one part of the Oz axis to other, during a cycle of the ac field can be observed even for $h^c_{ac,1} < h_{ac} < h^c_{ac,2}$ if the dimension of the particle is sufficiently small. Consequently, the induced signal m_{ac} does not have a rectangular-like form as in the case $T=0$ K and it is approximately in phase with the ac field, and its mean value over many cycles of the ac field is less than that obtained for $T=0$ K [see Fig. 12(a)]. Decreasing the dimension of the particle, the magnetic moment effectuates a considerable number of overbarrier rotations during a cycle of the ac field. Similar features are encountered for $\theta_k=89.9°$, but in this case, because the energy landscape is not symmetric, the higher energy minimum is less frequented by the magnetic moment and the induced signal is more distorted from its ideal sinusoidal form.

For $h_{dc} \leqslant h^*$ and $T=0$ K, the magnetic moment oscillates only around minimum 1 or minimum 2. However, for $T>0$ K, in continuance, the magnetic moment can pass from one part of the Oz axis to the other by means of the energy gained from the thermal field, the induced signal increases with the decrease of the dc field, and, consequently, the position of the anisotropy peaks moves toward smaller field values; that is, the effect of no-vanishing amplitude of the ac

field is amplified by the thermal agitation. When the dc field decreases, the energy minima become narrower and the amplitude of the random oscillations around the two minima decreases, the energy barriers increase, and the probability to pass from one minimum to other decreases, so that induced signal shifts into a rectangular-like form, and its amplitude increases exhibiting a maximum in the amplitude and, subsequently, in the phase shift behind the ac field [see Figs. 12(b)–12(d)].

At low values of h_{dc}, the magnetic moment oscillates close to the bottom of the energy minima, with the overbarrier relaxation mechanism being blocked and the induced signal is very small and in phase with the ac field.

The minimum of the imaginary TS [Eq. (12)] for the particles with the easy axis perpendicular to the dc field takes place when $2\kappa \simeq \omega$, that is, when the energy barrier in the absence of the ac field is $\Delta E^0/k_B T \simeq \ln(2f_0/\omega)$. From this relation, it can be seen that increasing the frequency of the excitatory ac field, the position of the imaginary TS peak moves toward higher dc field values, because increasing the frequency decreases the probability of surmounting the energy barrier. This increase is confirmed by our simulations. If $\tau=2\kappa$ is the relaxation time, then the above relation can be written as $\tau \simeq T_{ac}/2\pi$, where T_{ac} is the period of h_{ac}; that is, the minimum of the imaginary part [Eq. (12)] takes place when the relaxation time is 2π times smaller than the period T_{ac} of the ac field. In order to test this relation, we have counted in our numerical simulations the number of crossings of the magnetic moment of one particle from one part of the Oz axis to the other, and we have normalized it to the number of the cycles of the ac field, so that it does not depend on the number of cycles over which m_{ac} is averaged. For $T=0$ K, when h_{dc} decreases, the number of crossings n is equal to 1 until the norm of TS reaches its maximum value and is equal to 0 after that. Taking into account the temperature, the magnetization reversal can take place by thermal activation over the energy barriers, and when h_{dc} decreases, the number of crossing n decreases continuously from an infinite value (for $h_{dc}=1$ when there is no energy barrier) to 0 (when the energy barrier is very high and the probability of crossing is practically zero). In Fig. 13, presented are the number of crossings n_r when the real part of TS reaches its maximum value and the number of crossings n_i when the imaginary part reaches its minimum value as a function of particle's diameter. We can see that n_i increases from 1 to a limit value of approximately 2.2 as the particle's dimension decreases, while in the case of n_r, the increase is more abrupt. So, the micromagnetic analysis showed the complex behavior of the dynamics of the magnetic moment when the energy barrier is smaller than $k_B T$, the domain in which the two-level model is not valid.[37]

We note that the minimum values of the imaginary part and the phase shift do not take place for the same value of h_{dc}. The lag behind h_{ac} reaches the extreme value when the magnetic moment oscillates mainly around one minimum, but there is a small probability to pass from one minimum to another during a number of cycles of the ac field, so that $n<1$ [Fig. 12(d)]. So, the temperature has two antagonistic effects on the phase shift: for $h^* \leqslant h_{dc} \leqslant 1$, thermal fluctuations decrease the phase shift, while for $h_{dc} \leqslant h^*$, thermal fluctuations increase the phase shift.

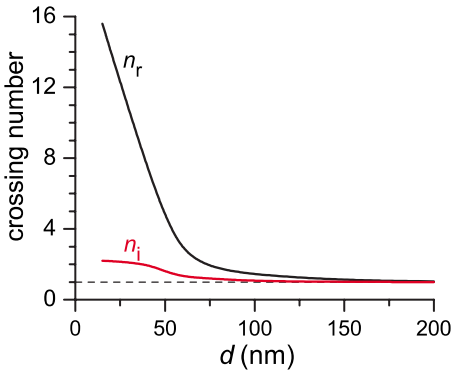

FIG. 13. (Color online) The number of crossings of the magnetic moment of one particle from one part of the Oz axis to the other, normalized to the number of the cycles of the ac field, as a function of particle's diameter: when the real part of TS reaches its maximum value (n_r) and when the imaginary part reaches its minimum value (n_i).

B. Particle distributions

From this point on, we are discussing the properties of a system of aligned particles lying in a regular network formed within one layer, the system being generated using lognormal distributions for volume and for the anisotropy constant. The results obtained for a noninteracting system are qualitatively similar of those obtained using the CP model. However, our results show the importance of the ac field amplitude. An increase of the most probable volume V_0 shifts TS's peaks to higher fields and sharpens the peaks. An increase of the most probable anisotropy constant K_0 also shifts the peaks to higher fields but their width increases. However, the width's relative variation is not so important in both cases. This fact is an important source of errors for the fitting procedure described in Refs. 19–22. The flattening of the volume distribution determines a decrease of imaginary TS and shifts its peak toward higher fields while its width increases (see Fig. 14). The most important factor in Eqs. (13) and (14) is σ_k: both the amplitude and the width of the TS peak strongly depend on it (see Fig. 14). As a consequence, σ_k is determined with the smallest errors by fitting procedure. By sys-

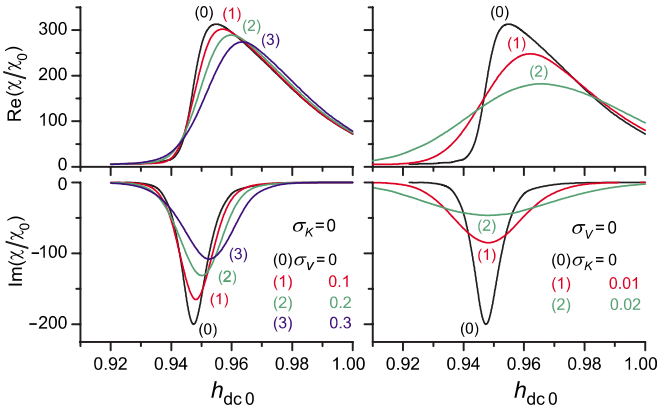

FIG. 14. (Color online) TS curves for different volume dispersions σ_V (left) and anisotropy dispersions σ_k (right) for $T=300$ K and $h_{ac0}^{max}=0.001$.

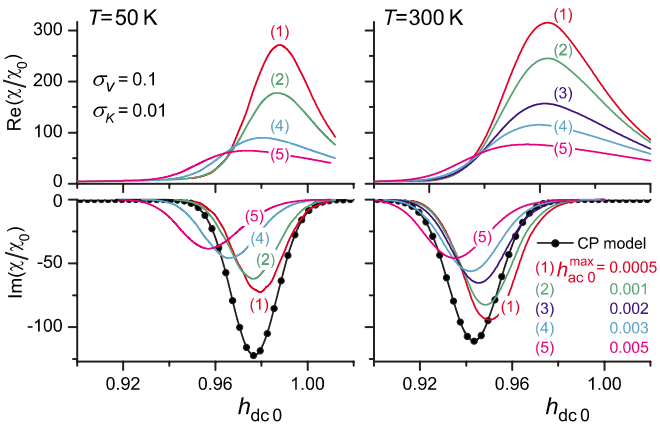

FIG. 15. (Color online) TS curves for σ_V=0.1, σ_k=0.01, and different values of the ac field amplitude for T=50 K (left) and T=300 K (right); with symbols, the curves predicted by the CP model are also presented.

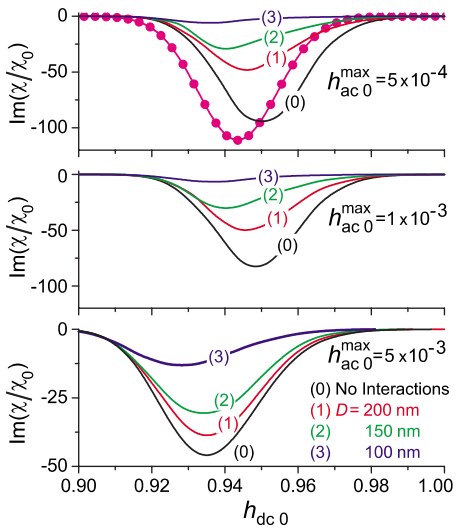

FIG. 16. (Color online) Imaginary TS curves for different values of the packing fraction and different values of the ac field amplitude (temperature T=300 K); with symbols, the curve predicted by the CP model is also presented.

tematic simulations, it was observed that a small angular dispersion of the easy axis affects the signal's amplitude only.

Figure 15 shows the ac field amplitude dependence of TS for two temperatures. The curves given by the CP model are also presented. We observe that only at low temperatures, as the ac field amplitude decreases, the CP model gives a better description of the results obtained with the SLLG equation. The effect of the increase of ac field amplitude is similar to a decrease of σ_V and V_0.

In order to see how the magnetostatic interactions between particles influence the TS curves, we have generated samples with increasing packing fraction. The magnetostatic interactions between particles are controlled by the network characteristic length D and periodic boundary conditions are used. The fast Fourier transform technique is applied in order to compute the field due to all particles. As the intensity of the interactions increases, the position of the imaginary TS peak moves toward smaller fields values (Fig. 16) and its amplitude decreases; that is, the effect of the interactions is somehow similar to the ac field amplitude.

In Ref. 34, a systematic quantitative analysis of the influence of the ac field amplitude and of the interactions between particles on the complex TS method for the determination of volume and anisotropy field distributions in perpendicular recording media is presented. Following a similar methodology as described in Refs. 19–22, we have fitted the "experimental" data produced by our micromagnetic model with the relation from the CP model. Because experimentally a signal proportional to the magnetization and not its real value is measured and because, as we mentioned in previous sections, the measured susceptibility is not equal to the differential susceptibility given by CP model, we have fitted the normalized imaginary TS curves even if in this way important information contained in the TS amplitude is lost. The most affected by the ac field amplitude and the interactions between particles are the volume distribution's parameters. In this case, the error generated by not taking into account the finite value of the ac field amplitude and by ignoring the interparticle interactions can be up to 55%. Similar results have been obtained for wider distributions, but the errors with which σ_V is obtained decrease if σ_V increases. However, for too large volume and anisotropy distributions, the peaks in the TS signal disappear. Assuming that the values of V_0 and K_0 are available through another measurement, we also tried to fit only σ_V and σ_k. In this case, the error with which σ_V is obtained increases because its effect is covered by the effect of the ac field amplitude.

VI. CONCLUSIONS

We have analyzed the origins of the imaginary part of TS: rate-independent hysteresis, viscous-type rate-dependent hysteresis, and thermal relaxation effect origin. The rate-independent origin is an intrinsic contribution to the imaginary TS and cannot be neglected because it is a zero-temperature effect. We have shown that because in the experimental procedure the amplitude of the ac field is not zero in the mathematical sense, a sinusoidal excitation gives rise to a distorted output, an irreversible susceptibility is measured, and the lag of the magnetization with respect to the applied field can be associated with a complex susceptibility. Starting from the energy loss per ac field cycle, an expression for the imaginary TS is obtained at T=0 K, assuming that in each moment the system lies in a minimum of the free energy. Also, using the critical curve formalism, we have shown how the ac field can induce a hysteresis and, consequently, imaginary TS. The magnetization dynamics in the framework of the LLG equation was used to analyze the occurrence of imaginary TS as a consequence of magnetization damping, which determines a lag between the magnetization's response and the applied excitation. This lag is strongly dependent on the excitation frequency. The model developed in Ref. 18, using a two-level approximation to take into account the temperature effects, was revised and certain clarifications and corrections have been made. Ther-

mal fluctuation effects on TS have also been considered using the stochastic LLG equation, and our results have been compared with those from Ref. 18, the differences between them being analyzed. The SLLG analysis showed complex behavior of the dynamics of the magnetic moment when the energy barrier is smaller than k_BT, the domain in which the two-level model is not valid.[37] We have shown that the thermal energy assists the switch discussed in the case $T=0$ K and causes a shift of the anisotropy peak toward lower field values and that the imaginary part of the TS is a cumulative effect of no-vanishing amplitude of the ac field, which is amplified by the thermal agitation. Finally, an analysis of the influence of the ac field amplitude and of the interactions between particles on the complex TS method for the determination of volume and anisotropy field distributions in perpendicular recording media, developed in Refs. 19–22, is presented.

ACKNOWLEDGMENTS

Work at AMRI was supported by DARPA under Grant No. HR0011-05-1-0031. This work was partially supported by Romanian CNCSIS under the Grant A (RELSWITCH).

APPENDIX

Let us consider a system of identical particles of volume V and uniaxial anisotropy of constant $K>0$, the easy axes being confined in the xOz plane, having the polar coordinate θ_k. The particle magnetization's spherical coordinates are denoted by (θ,φ) (see Fig. 8). The particle's free energy is given by

$$E=-2KV\left[h_{\mathrm{dc}}\cos\theta+h_{\mathrm{ac}}\sin\theta\cos(\varphi-\varphi_{\mathrm{ac}})+\frac{1}{2}(\sin\theta\cos\varphi\sin\theta_k+\cos\theta\cos\theta_k)^2\right],$$

and the necessary equilibrium condition,

$$\frac{\partial E}{\partial\theta}=0,\quad \frac{\partial E}{\partial\varphi}=0, \tag{A1}$$

has to be true for all h_{ac}. For $h_{\mathrm{ac}}=0$, the extreme points satisfy

$$\sin\varphi=0,$$

$$2h_{\mathrm{dc}}\sin\theta+\sin 2(\theta\mp\theta_k)=0, \tag{A2}$$

where "−" sign correspond to $\varphi=0$ and "+" to $\varphi=\pi$. It can be shown that there are two minima with $\varphi_1^0=0$ and $\varphi_2^0=\pi$ separated by a saddle point with $\varphi_3^0=\pi$. The polar angles corresponding to these three points are noted with θ_1^0, θ_2^0, and θ_3^0. The extreme points in the presence of a small ac field could be approximated by the first terms in the Taylor series expansions:

$$\theta_i(h_{\mathrm{ac}})\approx\theta_i^0+h_{\mathrm{ac}}\delta\theta_i,$$

$$\varphi_i(h_{\mathrm{ac}})\approx\varphi_i^0+h_{\mathrm{ac}}\delta\varphi_i,$$

where

$$\delta\theta_i=\lim_{h_{\mathrm{ac}}\to 0}\frac{d\theta_i}{dh_{\mathrm{ac}}}=\pm\frac{\cos\theta_i^0\cos\varphi_{\mathrm{ac}}}{\cos 2(\theta_i^0\mp\theta_k)+h_{\mathrm{dc}}\cos\theta_i^0}, \tag{A3}$$

$$\delta\varphi_i=\lim_{h_{\mathrm{ac}}\to 0}\frac{d\varphi_i}{dh_{\mathrm{ac}}}=\frac{\sin\varphi_{\mathrm{ac}}}{\cos(\theta_i^0\mp\theta_k)\sin\theta_k}, \tag{A4}$$

where the first sign corresponds to $i=1$ and the second to $i=2,3$. The variations $\delta\theta_i$ and $\delta\varphi_i$ are obtained by differentiating relations (A1) with respect to h_{ac}. When the energy barriers ΔE are very small in comparison with k_BT (k_B is the Boltzmann constant and the T is the temperature), the thermal agitation causes continual changes in the orientation of the magnetic moment. When $\Delta E/k_BT$ is large enough, a discrete-orientation model can be used: if the occupation probabilities of the two energy levels are denoted by n_1 and $n_2=1-n_1$ and if a particle in orientation i has probability κ_{ij} per unit time of jumping to orientation j, then the approach to statistical equilibrium is described by the following master equation:

$$\frac{dn_1}{dt}=-\kappa_{12}n_1+\kappa_{21}n_2. \tag{A5}$$

The rates of thermally activated transitions of noninteracting particles are generally assumed to be given by the Néel-Brown (or Arrhenius) expression

$$\kappa_{ij}=f_0\exp\left(-\frac{E_3-E_i}{k_BT}\right), \tag{A6}$$

where E_1 and E_2 are the energies of the two local minima, and E_3 is the energy of the saddle point separating them. This simple model breaks down as $\Delta E/k_BT$ decreases, because the distribution of the particle orientation will no longer be sufficiently concentrated near the two minima. Aharoni[37] has shown, in the case of uniaxial anisotropy and zero magnetic field, that the high-energy-barrier approximation is still a good approximation when the barriers are of the order of k_BT. However, when the dc field is in the vicinity of H_k, the energy barrier becomes very small in comparison with k_BT.

In the presence of the ac field on besides the explicit time dependence of the occupation probabilities, there is an implicit time dependence via ac field, $n_1(h_{\mathrm{ac}}(t),t)$, and in first approximation, we can write

$$n_1(h_{\mathrm{ac}}(t),t)\approx n_1(0,t)+h_{\mathrm{ac}}(t)\delta n_1(t), \tag{A7}$$

where $\delta n_1(t)=\partial n_1(0,t)/\partial h_{\mathrm{ac}}$. The normalized magnetic moment along the ac field is

$$\begin{aligned}m_{\mathrm{ac}}(h_{\mathrm{ac}}(t),t)=n_1(h_{\mathrm{ac}}(t),t)&\sin\theta_1(h_{\mathrm{ac}}(t))[\cos\varphi_1(h_{\mathrm{ac}}(t))\cos\varphi_{\mathrm{ac}}\\&+\sin\varphi_1(h_{\mathrm{ac}}(t))\sin\varphi_{\mathrm{ac}}]\\&+n_2(h_{\mathrm{ac}}(t),t)\sin\theta_2(h_{\mathrm{ac}}(t))\\&\times[\cos\varphi_2(h_{\mathrm{ac}}(t))\cos\varphi_{\mathrm{ac}}\\&+\sin\varphi_2(h_{\mathrm{ac}}(t))\sin\varphi_{\mathrm{ac}}],\end{aligned}$$

which gives for the TS the expression

$$\chi = \lim_{h_{ac}\to 0} \frac{\partial m_{ac}(h_{ac}(t),t)}{\partial h_{ac}}$$
$$= (\sin\theta_1^0 + \sin\theta_2^0)\cos\varphi_{ac}\delta n_1(t) + [(\cos\theta_1^0\delta\theta_1 + \cos\theta_2^0\delta\theta_2)\cos\varphi_{ac} + (\sin\theta_1^0\delta\varphi_1 + \sin\theta_2^0\delta\varphi_2)\sin\varphi_{ac}]n_1(0,t) - \cos\theta_2^0\cos\varphi_{ac}\delta\theta_2 - \sin\theta_2^0\sin\varphi_{ac}\delta\varphi_2. \quad \text{(A8)}$$

The master equation [Eq. (A5)] describing the time evolution of the occupation probability of the first energy minimum is

$$\frac{dn_1(h_{ac}(t),t)}{dt} = -[\kappa_{12}(h_{ac}(t)) + \kappa_{21}(h_{ac}(t))]n_1(h_{ac}(t),t) + \kappa_{21}(h_{ac}(t)), \quad \text{(A9)}$$

and in first approximation, one can write

$$\kappa_{ij}(h_{ac}(t)) \approx \kappa_{ij}(0) + h_{ac}(t)\delta\kappa_{ij},$$

$$E_i(h_{ac}(t)) \approx E_i(0) + h_{ac}(t)\delta E_i,$$

where

$$\delta\kappa_{ij} = \frac{d\kappa_{ij}(0)}{dh_{ac}} = -\kappa_{ij}(0)\frac{\delta E_3 - \delta E_i}{k_B T}, \quad \text{(A10)}$$

$$\delta E_i = \frac{dE_i(0)}{dh_{ac}} = \mp 2\sin\theta_i^0\cos\varphi_{ac}KV. \quad \text{(A11)}$$

In the above relations, it is assumed that the magnetic moment is only in an extreme of the free energy and there is no distribution of the particles' orientation around minima due to thermal fluctuations, and the energy is taken as a function of h_{ac} only. For brevity, in the what follows, we shall note with superscript "0" the values of different quantities at $h_{ac}=0$. Thus, in first approximation, the master equation [Eq. (A9)] can be written as

$$\frac{dn_1(h_{ac}(t),t)}{dt} = -(\kappa_{12}^0 + \kappa_{21}^0)n_1^0(t) + \kappa_{21}^0 + h_{ac}(t)[-(\kappa_{12}^0 + \kappa_{21}^0)\delta n_1(t) + \delta\kappa_{21} - (\delta\kappa_{12} + \delta\kappa_{21})n_1^0(t)]. \quad \text{(A12)}$$

Using the approximation

$$\frac{dn_1(h_{ac}(t),t)}{dt} \approx \frac{dn_1^0(t)}{dt} + h_{ac}(t)\frac{d(\delta n_1(t))}{dt} + \frac{dh_{ac}(t)}{dt}\delta n_1(t)$$

and with $\mathbf{h}_{ac}=\mathbf{h}_{ac,max}\exp(i\omega t)$, Eq. (A12) turns into

$$\frac{d(\delta n_1(t))}{dt} = -(\kappa_{12}^0 + \kappa_{21}^0 + i\omega)\delta n_1(t) + \delta\kappa_{21} - (\delta\kappa_{12} + \delta\kappa_{21})n_1^0(t).$$

Neglecting the time dependence of n_1^0 and with initial condition $\delta n_1(0)=0$, one obtains

$$\delta n_1(t) = [e^{-(\kappa_{12}^0+\kappa_{21}^0)t}e^{-i\omega t} - 1]\frac{(\delta\kappa_{12} + \delta\kappa_{21})n_1^0 - \delta\kappa_{21}}{\kappa_{12}^0 + \kappa_{21}^0 + i\omega}.$$

In view of the exponential variation of transition rates [Eq. (A6)], the first term from the second member can be neglected when the energy barrier is comparable with k_BT. Using Eqs. (A10) and (A11), one obtains

$$\delta n_1(t) = \beta\frac{(\kappa_{12}^0 g_1 + \kappa_{21}^0 g_2)n_1^0 - \kappa_{21}^0 g_2}{\kappa_{12}^0 + \kappa_{21}^0 + i\omega},$$

where $g_i=(\delta E_3-\delta E_i)/KV$. Because the time dependence of n_1^0 is neglected, we have $-(\kappa_{12}^0+\kappa_{21}^0)n_1^0+\kappa_{21}^0=0$, and thus the real and imaginary components of Eq. (A8), using Eq. (A2), can be written as

$$\chi_r = \begin{cases} \beta(\sin\theta_1^0 + \sin\theta_2^0)\cos\varphi_{ac}\dfrac{\kappa_{12}^0\kappa_{21}^0(g_1-g_2)}{\omega^2 + (\kappa_{12}^0+\kappa_{21}^0)^2} & \\ \quad + [(\cos\theta_1^0\delta\theta_1 + \cos\theta_2^0\delta\theta_2)\cos\varphi_{ac} + (\sin\theta_1^0\delta\varphi_1 + \sin\theta_2^0\delta\varphi_2)\sin\varphi_{ac}]n_1^0 & \\ \quad - \cos\theta_2^0\cos\varphi_{ac}\delta\theta_2 - \sin\theta_2^0\sin\varphi_{ac}\delta\varphi_2, & \text{if } h_{dc} < h_{cr}(\theta_k) \\ \cos\theta_1^0\cos\varphi_{ac}\delta\theta_1 + \sin\theta_1^0\sin\varphi_{ac}\delta\varphi_1, & \text{if } h_{dc} \geq h_{cr}(\theta_k), \end{cases} \quad \text{(A13)}$$

$$\chi_i = \begin{cases} \beta(\sin\theta_1^0 + \sin\theta_2^0)\cos\varphi_{ac}\omega\dfrac{\kappa_{12}^0 g_2 - (\kappa_{12}^0 g_1 + \kappa_{21}^0 g_2)n_1^0}{\omega^2 + (\kappa_{12}^0+\kappa_{21}^0)^2}, & \text{if } h_{dc} < h_{cr}(\theta_k) \\ 0, & \text{if } h_{dc} \geq h_{cr}(\theta_k), \end{cases} \quad \text{(A14)}$$

where

$$h_{cr}(\theta_k) = (\sin^{2/3}\theta_k + \cos^{2/3}\theta_k)^{-3/2}$$

is the critical field [for an orientation θ_k of the easy axis, there are two minima of the free energy when $h_{dc} < h_{cr}(\theta_k)$]. These two equations are equivalent to Eqs. (11) and (12) from Ref. 18.

For $\theta_k = 90°$ and $-1 < h_{dc} < 1$, we have $E_1^0 = E_2^0 = -(1+h_{dc}^2)KV$, $E_3^0 = -2h_{dc}KV$, and $\kappa_{12}^0 = \kappa_{21}^0 = \kappa = f_0 \exp[-\beta(1-h_{dc})^2]$, so that the complex susceptibility is given by Eqs. (11) and (12).

*Permanent address: Faculty of Physics, "Al. I. Cuza" University, Iasi 700506, Romania.
†LSpinu@uno.edu

[1] P. Poddar, J. L. Wilson, H. Srikanth, D. F. Farrell, and S. A. Majetich, Phys. Rev. B **68**, 214409 (2003).
[2] P. Vavassori, D. Bisero, F. Carace, A. di Bona, G. C. Gazzadi, M. Liberati, and S. Valeri, Phys. Rev. B **72**, 054405 (2005).
[3] L. Spinu, A. Stancu, Y. Kubota, G. Ju, and D. Weller, Phys. Rev. B **68**, 220401(R) (2003).
[4] L. Spinu, H. Srikanth, A. Gupta, X. W. Li, and G. Xiao, Phys. Rev. B **62**, 8931 (2000).
[5] N. A. Frey, S. Srinath, H. Srikanth, M. Varela, S. Pennycook, G. X. Miao, and A. Gupta, Phys. Rev. B **74**, 024420 (2006).
[6] D. Kechrakos and K. N. Trohidou, Phys. Rev. B **74**, 144403 (2006).
[7] R. Gans, Ann. Phys. **29**, 301 (1909).
[8] A. Aharoni, E. H. Frei, S. Shtrikman, and D. Treves, Bull. Res. Counc. Isr., Sect. A: Math., Phys. Chem. **6A**, 215 (1957).
[9] L. Pareti and G. Turilli, J. Appl. Phys. **61**, 5098 (1987).
[10] J. J. Lu, H. L. Huang, C. R. Chang, and I. Klik, J. Appl. Phys. **75**, 5499 (1994).
[11] J.-S. Yang, C.-R. Chang, and I. Klik, Phys. Rev. B **51**, 15203 (1995).
[12] L. Spinu, A. Stancu, and C. J. O'Connor, Appl. Phys. Lett. **80**, 276 (2002).
[13] I. Dumitru, A. Stancu, D. Cimpoesu, and L. Spinu, J. Appl. Phys. **97**, 10E304 (2005).
[14] L. Spinu, I. Dumitru, A. Stancu, and D. Cimpoesu, J. Magn. Magn. Mater. **296**, 1 (2006).
[15] D. Cimpoesu, A. Stancu, and L. Spinu, J. Nanosci. Nanotechnol. (to be published).
[16] L. Spinu, H. Srikanth, E. E. Carpenter, and C. J. O'Connor, J. Appl. Phys. **87**, 5490 (2000).
[17] L. Spinu, H. Pham, C. Radu, J. C. Denardin, I. Dumitru, M. Knobel, L. S. Dorneles, L. F. Schelp, and A. Stancu, Appl. Phys. Lett. **86**, 012506 (2005).
[18] C. Papusoi, Jr., Phys. Lett. A **265**, 391 (2000).
[19] G. P. Ju, R. Chantrell, H. Zhou, D. Weller, and B. Lu, *Digest of Intermag 2003* (IEEE, New York, 2003), p. FE-01.
[20] G. P. Ju, R. Chantrell, H. Zhou, and D. Weller, U.S. Patent No. 2004/0066190 A1 (8 April 2004).
[21] G. P. Ju, H. Zhou, R. Chantrell, B. Lu, and D. Weller, J. Appl. Phys. **99**, 083902 (2006).
[22] G. P. Ju, B. Lu, R. J. M. van de Veerdonk, X. Wu, T. J. Klemmer, H. Zhou, R. Chantrell, A. Sunder, P. Asselin, Y. Kubota, and D. Weller, IEEE Trans. Magn. **43**, 627 (2007).
[23] E. Yuan and R. H. Victora, IEEE Trans. Magn. **40**, 2452 (2004).
[24] J. I. Gittleman, B. Abebes, and S. Bozowski, Phys. Rev. B **9**, 3891 (1974).
[25] G. Bertotti, *Hysteresis in Magnetism: For Physicists, Materials Scientists, and Engineers* (Academic, San Diego, 1998).
[26] R. W. Chantrell, A. Hoare, D. Melville, H. J. Lutke-Stetzkamp, and S. Methfessel, IEEE Trans. Magn. **25**, 4216 (1989).
[27] A. Thiaville, J. Magn. Magn. Mater. **182**, 5 (1998).
[28] A. Thiaville, Phys. Rev. B **61**, 12221 (2000).
[29] S. E. Russek, P. Kabos, T. Silva, F. B. Mancoff, D. Wang, Z. Qian, and J. M. Daughton, IEEE Trans. Magn. **37**, 2248 (2001).
[30] G. V. Skrotskii and L. V. Kurbatov, Sov. Phys. JETP **35**, 148 (1959); *Ferromagnetic Resonance*, edited by S. V. Vonsovskii (Pergamon, Oxford, 1966), p. 19.
[31] T. L. Gilbert, Phys. Rev. **100**, 1243 (1955).
[32] W. F. Brown, Jr., Phys. Rev. **130**, 1677 (1963).
[33] D. Cimpoesu, A. Stancu, I. Dumitru, and L. Spinu, IEEE Trans. Magn. **41**, 3121 (2005).
[34] D. Cimpoesu, A. Stancu, and L. Spinu, IEEE Trans. Magn. **42**, 3153 (2006).
[35] D. Cimpoesu, A. Stancu, and L. Spinu, J. Appl. Phys. **99**, 08G105 (2006).
[36] P. E. Kloeden and E. Platen, *Numerical Solution of Stochastic Differential Equations* (Springer, Berlin, 1995).
[37] A. Aharoni, Phys. Rev. **135**, A447 (1964).